CCUS: 4015008

EXPERIMENTAL STUDY OF BRINE COMPATIBILITY ON WATER-ALTERNATING-CO_2 INJECTION IN LOW-PERMEABILITY MORROWAN SANDSTONE RESERVOIR

Anthony Morgan[1,2], William Ampomah[1], Robert Czarnota*[1], Sai Wang[1], Reid Grigg[1], Jiawei Tu[1], 1. Petroleum Recovery and Research Center, New Mexico Tech, Socorro, New Mexico, USA, 2. Petroleum and Natural Gas Department, University of Energy and Natural Resources, Sunyani, Ghana.

Abstract

Brine incompatibility is an intricate issue overshadowing the success of water-alternating-gas (WAG) enhanced oil recovery (EOR) project. Its effect is especially noted in uncontrolled Low salinity (Lowsal) waterflood-operated fields. In this study, the inefficient waterflooding in a low permeable Morrowan sandstone is investigated through a comprehensive experimental study. The implications concluded from this study are critical for improving the efficiency of CO2-WAG EOR and Sequestration with compatible brine injection. This in part was conducted through Core-flood experiments, fluid-fluid surface charge, compatibility, and rock-fluid interactions analysis. Stable electrostatic forces prevent in a solution prevents particle aggregation, but distortion in surface charges weakens the expulsion forces and causes precipitation. Surface charge and compatibility tests revealed fluid-fluid reactivity and scale formation influenced by high ionic concentrations differences, temperature, and pressure. Fluid-fluid mixtures with produced water exhibited a unique compatibility signature, with a transition point causing of increasing and decreasing turbidity and vice-versa for ζ-potential (zeta potential) respectively. Geochemical analysis indicated precipitation of aragonite, calcite, and dolomite under reservoir conditions. Rocks interacted differently with synthetic brine, showing intense surface activity with low salinity water. Element-mineral associations showed clays and mineral particles obstructing pores and pore throats. In summary, the principal mechanisms of waterflood failure include low permeability, mineral composition (especially clay minerals), clay mineral reactivity, increased pressure drop (ΔP), fluid-fluid reactivity. These factors collectively contribute to formation damage, pore plugging, reduced flow capacity, and ultimately the failure of waterflood operations. This study thus, provide a new dataset from a Morrowan-aged clastic reservoir in the Anadarko basin offering insights into waterflood response. This knowledge will aid in optimizing brine composition for CO_2-WAG EOR or an informed decision on the type of improved recovery to employ.

Keywords: Inefficient waterflood, uncontrolled salinity, surface charge geochemistry, low permeability, zeta potential, electrical conductivity, Morrowan sandstone-Farnsworth Unit.

1.0 Introduction

The success of EOR techniques depends on major factors as the properties of the in-situ fluid and the geological and mineralogical characterization of the reservoir and most importantly a detailed insight into

the performance of previous secondary recovery techniques (especially waterflooding). Noticeable among EOR techniques is gas injection, which utilizes gas such as natural gas, nitrogen or carbon dioxide as injectants and accounts for about 60% of U.S. EOR oil production [1]. CO_2-EOR is currently one of the most attractive and matured EOR techniques not only for its efficiency in oil recovery but also in the reduction of global warming coupled with incentives to operators for tons of CO_2 sequestered. CO_2-EOR could be extended to include a water injection scheme, where injected gas is alternated with the injection of water to reduce the mobility contrast between gas and reservoir oil, i.e. water alternating gas (WAG) EOR [2]. In this scenario, two techniques (water flooding and gas injection) are therefore coupled together for an increment in recovery. Continuous gas injection (CGI) improves microscopic displacement efficiency but factors such as gravity segregation and viscous fingering of CO_2 in high permeable zones, makes CO_2-WAG more efficient, because it increases oil recovery to about 5% more than CGI [3]. Alternating gas with water increases macroscopic sweep efficiency through mobility control and also builds up reservoir pressure to increase miscibility of injected gas and reservoir oil [2]. However, the application of waterflood may not produce the desired effect on every reservoir as has been recorded in several studies. Thus, a comprehensive investigation ought to be undertaken into the mechanistic factors governing waterflood pre or post performance. This will provide an informed decision criteria for operators on the type of improved recovery technique, especially for considerations towards CO_2-WAG deployment.

The eastern section of the Farnsworth Unit (FWU) (Figure 1) in Texas experiences an inefficient waterflood, contrasting with the efficient operation on the west side. Despite sharing the same geological characteristics, the east exhibits higher estimated oil initially in place (OIIP) and primary production. Successful waterflood in the west prompted consideration of CO_2-WAG enhanced oil recovery and storage which is currently ongoing. The study's objective is to decipher the mechanisms behind waterflood inefficiency through core flood experiments. Additional tests, such as core-fluid compatibility, XRD, scanning electron micrographs, turbidity, and ζ-potential (zeta potential) measurements, aim to identify clay effects and mineral composition changes, providing a comprehensive understanding of waterflood inefficiency in the FWU's eastern section. This will enable an informed decision on the type of improved recovery technique to be employed, specifically CGI and WAG utilizing CO_2 as the working gas phase fluid. This paper focuses on utilizing surface charge geochemistry building on previous studies [4], [5] where fluid-fluid and rock-fluid interaction were analyzed to develop compatibility signature for FWU.

2.0 A General Overview and Operations of FWU

The discovery of FWU traces back to 1955. The field is located in the Pennsylvanian-age system in the northwest part of the Anadarko basin in Ochiltree County, Texas [6]–[10]. This geological system consists of sandstone and mudstone sequences [11], [12][9], [13]. Particular interest is the Morrow B reservoir from the Morrowan period, characterized by limestones intercalated with mudstones and coal that formed in an incised-valley filled during a fluvial low stand and marine transgression (Figure 1). The impact of primary deposition characteristics on reservoir performance is found to be less significant compared to diagenetic features. Notable diagenetic alterations include feldspar modification and the formation of authigenic clays, influencing porosity changes. Dissolution of silica, quartz, calcite, and siderite cementation, along with minor pyrite formation, are observed [11][14], [15][16]–[18]. The Morrow formation spans from 7550ft to 7950ft depths, and is predominantly composed of subarkosic sandstone with chlorite, smectite, siderite, dolomite, calcite, illite, and kaolinite introduced by diagenetic processes. The reservoir is confined by mineral and stratigraphic trapping mechanisms, with Morrow shales acting as primary seals. The Morrow formation is described as a heterogeneous reservoir with four principal lithofacies (fine-grained sandstone, coarse-grained sandstone, conglomerate, and mudstone) further subdivided into seven subfacies [11]. The dominant porosity facies include grained-sized pores and micro-porous clays.

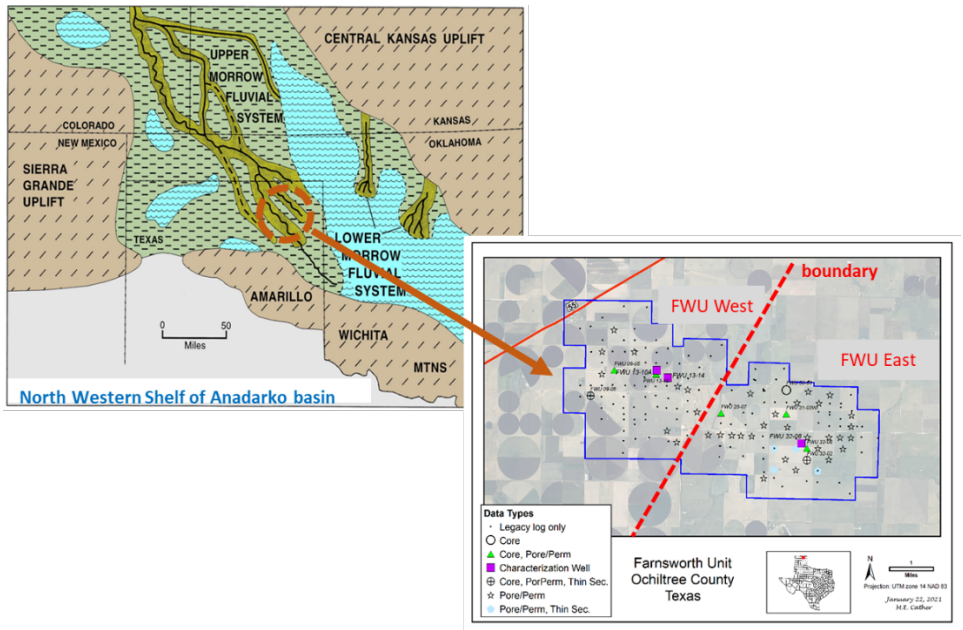

Figure 1: paleographic image of Morrow and site map of FWU modified from [15], [19]

3.0 Data and methods

The primary objective of this study was to investigate the potential mechanisms of waterflood failure in the east section of FWU using an experimental approach. The experiment was conducted in two parts. Firstly, a fluid-fluid test was performed to assess the compatibility of connate and injection water under both ambient and reservoir conditions. Secondly, a rock-fluid analysis was carried out, which involved a core flow test using single-phase brine flow test. These tests aimed to analyze the interaction between the rock and injected fluids and their impact on the storage and flow capacity of the core samples, which were simulated to replicate initial reservoir conditions. Detailed procedures, materials, and equipment utilized are presented in the subsequent sections of this chapter. Analyzed properties of core samples from variable depths of the reservoir are summarized in Table 1.

Table 1: Properties of Core sample measured.

Depth in res./ ft	Core plug ID	L/in	D/in	M(dry)/g	M(wet)/g	PV	porosity, %	Permeability/, Md
	A	1	1.45	66.76	69.50	2.74	10.13	0.15
7967	B	1.19	1.45	82.88	85.00	2.12	6.58	0.108
	C	1.25	1.45	78.59	81.00	2.41	7.12	0.121
	D	1.26	1.45	82.74	85.10	2.36	6.92	0.107
7969	E	1.19	1.45	79.66	82.30	2.64	8.20	0.186
	F	1.25	1.45	78.1	81.00	2.9	8.57	0.191
7973	G	1.31	1.45	82.92	85.60	2.68	7.56	0.13

7974	H	1.24	1.45	80.89	83.50	2.61	7.78	0.131
	I	1.25	1.45	76.25	79.00	2.75	8.13	0.183
	J	1.31	1.45	86.58	89.00	2.42	6.83	0.124
	K	1.09	1.45	68.03	71.00	2.97	10.07	0.77
	L	1.13	1.45	72.93	75.20	2.27	7.42	0.104
	M	1.25	1.45	78.8	81.00	2.2	6.50	0.11
	N	1.19	1.45	74.2	77.00	2.8	8.70	0.152

3.1 Synthetic Brine formulation

The ionic compositions of connate water in the Morrow reservoir within the Anadarko Basin were obtained from [20], and the fresh water from the Ogallala aquifer and produced water compositions reported were obtained from [21]. Table 2 presents the reported compositions of the brine used in the study. The brine was synthesized using the following chemicals: Sodium Chloride (NaCl), Sodium Sulfate (Na2SO4), Magnesium Chloride (MgCl2), Calcium Chloride (CaCl2), Sodium Bicarbonate (NaHCO3), Potassium Chloride (KCl), Aluminum Chloride (AlCl3), and Ferrous Sulfate Hepta-hydrate (FeSO4.7H2O). To prepare the brine, distilled water (approximately 3 ppm) was used. The required mass of each compound was determined in order to represent the desired aqueous speciation of the synthesized brine. The required mass of each compound was determined in order to represent the desired aqueous speciation of the synthesized brine. The calculation of the mass, involved the following steps:

(i) Molar masses (g/mol) of the various compounds were determined;

(ii) Concentrations were converted from mg/L to g/L [g/L = (mg/L)/1000];

(iii) Moles per each ion was calculated (multiply volume of solution required in liters), [Moles = concentration (g/L) *(volume of solution, L)/Molar mass (g/mol)];

(iv) Stoichiometry was utilized in determining moles of each compound; and

(v) Mass of compound is estimated using the stoichiometric moles and the molar mass of each compound, [Mass = moles * molar mass].

Table 2: Aqueous species/ionic composition

Aqueous Species	Avg. Connate Water (mg/L)	Fresh Water Concentration (mg/L)	Produced Water Concentration (mg/L)
Na+	2.25E+04	4.53E-01	1.29E+03
Ca2+	4.25E+03	1.52E-02	3.69E+01
Mg2+	6.75E+02	1.64E-03	9.60E+00
K+	-	3.11E-04	7.74E+00
Fe2+	-	-	3.77E-05
Al3+	-	-	5.48E-01

HCO3-	5.00E+02	2.96E+01	3.03E+04
Cl-	4.05E+04	4.49E-01	1.71E+03
SO42-	2.35E+03	2.40E-03	1.78E+01
pH	6.54E+00	7.00E+00	7.00E+00

3.3 Fluid-Fluid compatibility and surface charge test

Connate water or formation water (SCW) and injection water (SIIW) were tested for possible mineral dissolution and precipitation. These were conducted at ambient conditions (70 ^{o}F) and at reservoir pressure of 2000 psi and temperature of 125 ^{o}F in a PVT cell. Three sets of compositions were mixed at variable proportion in a 15 ml centrifuge conical tubes: freshwater -connate water (FC), produced water – connate water (PC) and freshwater – produced water (FP) mixtures. The mixing ratios ranged from (20:80)%, (40:60)%, (50:50)%, (60:40)% and (80:20)%. After a period of injection, produced water concentration now becomes the stabilized reservoir water saturation. The further injection of fresh water or any other composition may further cause instability or incompatibility. Hence the analysis of produced water as a different brine salinity and composition. The mixtures were stored for 7 days and observed for changes in clarity and solid formation. Turbidity (using the vernier turbidity sensor) of the mixtures were tested after which they were filtered for any precipitates. Total dissolved salts (salinities), pH, electrical conductivity and ζ-potential tests were conducted to assess the solution stability and compatibility.

3.4 Tests conducted and Equipment utilized

To simulate reservoir conditions, a high-temperature-high-pressure (HTHP) pressure-volume-temperature (PVT) cell was employed. This cell is connected to a data acquisition (DAQ) system with signal processing transducers that can be controlled remotely using LABVIEW software. For turbidity and salinity measurements, Vernier turbidity and TDS (Total Dissolved Solids) sensors were utilized. These sensors operate in conjunction with a computer software called Logger Pro. The turbidity sensor was calibrated using a two-point calibration routine, where a 100 NTU (Nephelometric Turbidity Unit) standard turbidity fluid and distilled water (0 NTU) were used in a cuvette. Approximately 100 measurements were recorded, and the mean value was taken as the final value to ensure greater stability and accuracy. The turbidity sensor measures light scattering caused by particles in suspension. A turbidity value of 0 NTU indicates a very clear solution, while higher values indicate increasing levels of cloudiness or the presence of particles in suspension. The TDS sensor was also calibrated using a one-point calibration routine, employing a 35ppt (parts per thousand) solution as a reference. ζ-Potential measurements of samples were conducted with Anton Paar Litesizer 500 linked to a Kalliope computer program. The instrument employs the Laser Doppler electrophoresis (LDE) technique in acquiring the ζ-Potential of suspended particles. The stability and behaviors of suspended particulates can be inferred from particle's surface electro-kinetic potential (ζ-Potential). This gives information about inter-particle interaction, dispersive characters, and flocculation susceptibilities. ζ-potential measurements are important in understanding rock-brine interactions in oil and gas enhanced recovery. They determine surface charge, predict particle aggregation and dispersion, and help assess colloidal system stability, mineral scaling, corrosion potential, and ion adsorption. ζ-potential has been instrumental in optimizing enhanced oil recovery techniques by understanding how reservoir rocks behave with low salinity brine. It contributes to a better understanding of electrochemical phenomena, fluid flow, scaling tendencies, and effective EOR strategies, making it valuable in many fields.

3.5 PH Redox Equilibrium in Complex Groundwater Systems (PHREEQC)

PREEQC is an aqueous system geochemical reactions modeling software developed by the United States Geological Survey (USGS). Its application is particularly for analyzing groundwater and natural water chemistry as well as hydrothermal systems. It employs thermodynamics to estimate the speciation and distribution of chemical species based on the pH, temperature and pressure of the system. A command driven interface and scripting program for batch process and cumbersome simulations. In this study,

PHREEQC was utilized to perform series of geochemical simulations to investigate the diagenetic reaction between the mixing of reservoir connate water and various compositions of injection water. Figure 2 represents the workflow utilized for the simulation.

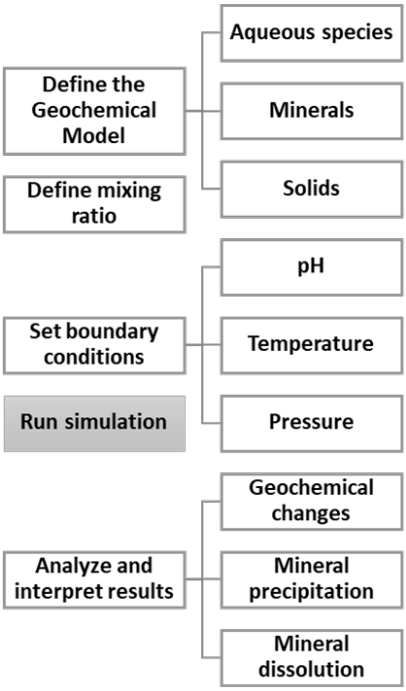

Figure 2: PHREEQC geochemical reaction workflow

4.0 Results

4.1 Fluid – Fluid Compatibility and Surface Charge

Figure 3 represents results of core flow-through experiment with variable salinities. It is observed that permeability decreases with an increase in differential pressure (ΔP) as salinity decreases to low salinity (LS). The measured permeabilities also indicate very low permeability values on the eastside of the reservoir as compared to the westside (as seen in preliminary analysis, Figure 4). The mechanisms associated with the success or failure of waterflood are however, not limited to the rock and fluid interactions in sandstone reservoirs. In most cases, connate water composition and salinities are different from injection fluids. Hence the compatibility of injection water during waterflood operation is paramount. Incompatible connate and injection water may lead to dissolution and precipitation issues, and impair reservoir storage and flow capacity. This section investigates as part of factors leading to inefficiency on FWU-east, two different injection water compositions and connate water mixtures at different proportions at ambient and reservoir conditions. The prepared samples were stored for 7 days after which measurements were taken.

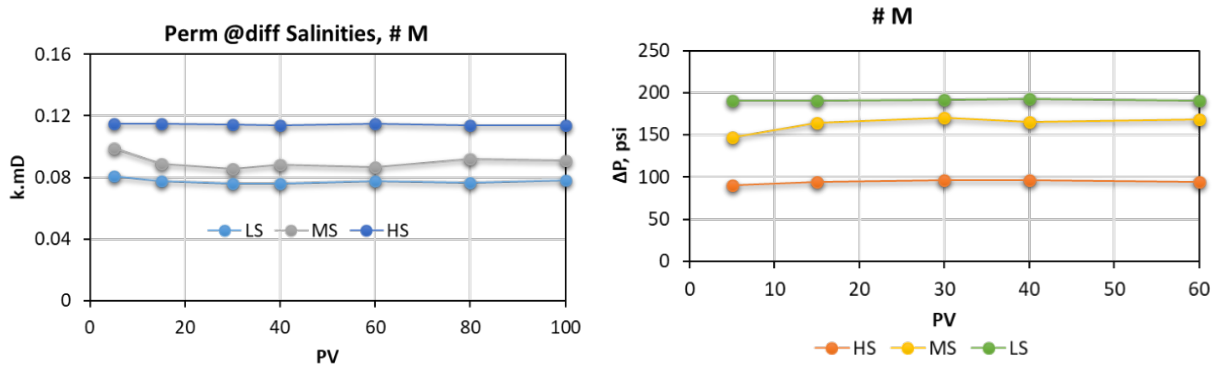

Figure 3: Comparative analysis of permeability and ΔP values at variable PV injected for different brine salinity

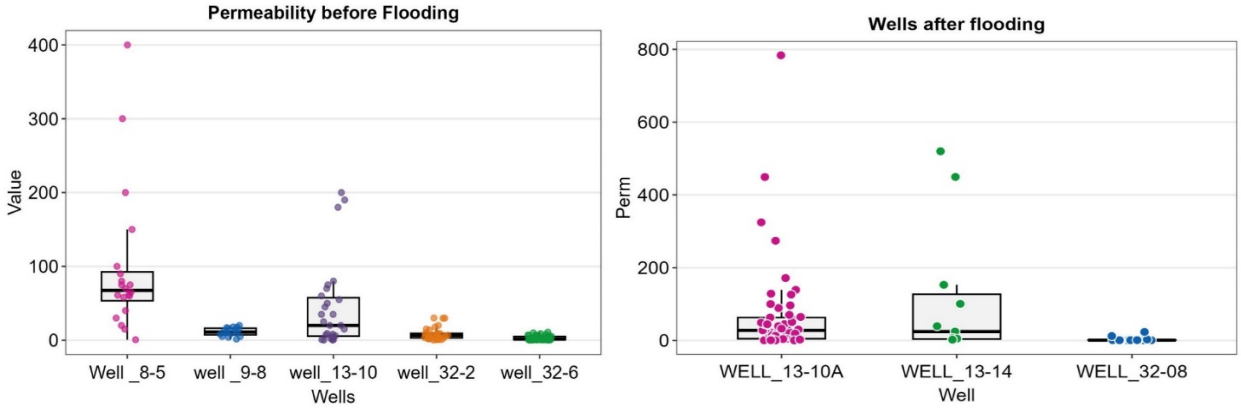

Figure 4: Permeability values (mD) before flooding, from: East (well_32-2, well_32-6) , West (well_8-5, well_9-8 and well_13-10) and after flooding, from: East (well_32-08), West (well_13-10A, well_13-14,)

Figure 5(a) presents pH and TDS measurements of freshwater (SIIW (LS)) and connate (SCW) mixtures. pH_Before and pH_After generally increases as the proportion of freshwater increases with a decrease in TDS. With respect to individual mixtures, pH and TDS after 7 days show relatively reduced values as depicted in Figure 5(a). From 5(b) the corresponding turbidity measurements reduces in ascending order of SIIW-LS proportion, whiles conductivity decreases in that regard. However, ζ-potential decreases or the surface charge or potential of the mixtures after 7 days become more negatively charged with an increase in %volume of SIIW. The results of LS-SIIW and synthetic production water (SPW) are reported in Figure 6(a) and Figure 6(b). Ph and TDS before and after 7 days exhibit the same trend as recorded in LS (SIIW and) HS (SCW) mixtures. Turbidity and ζ-potential follow a different trend. There is an increase in turbidity with a corresponding decrease in ζ-potential (negative charge) until a 50 – 50% mixture (from 80% SPW to 50% SPW). From 60% LS to 80% LS turbidity declines with an increase in ζ-potential. In this mixture turbidity and ζ-potential are strongly influenced by the proportions of ionic concentrations of the two solutions above or below 50th percent volume.

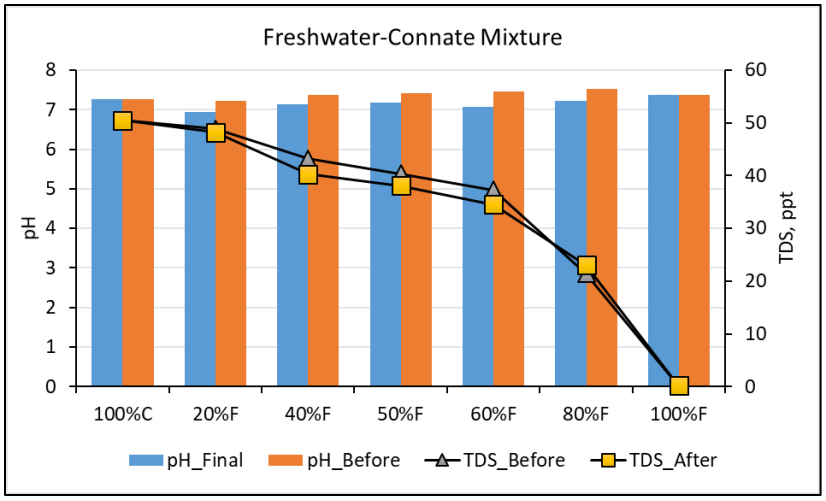

Figure 5(a): PH and TDS readings for LS (SIIW) and HS (SCW) mixtures.

TDS, Ph, and conductivity (Figure 17a, 17b) repeats a similar trend as described mixtures above for SPW and SCW mixtures. Turbidity also increases and declines until the midpoint mixture as exhibited in SPW and SCW mixtures ζ-potential however increases towards the negative charge as volume of SPW increases from 20% to 80% (Figure 17b). This trend in turbidity only happens in mixtures involving SPW. At an equal ratio 50:50 mixture turbidity is at its peak, but reduces towards which side of the ratio increases. This is also repeated for ζ-potential values, which reduces or increases towards the 100% values of the original solutions forming the mixture. The mixtures of SIIW – SCW and SPW – SCW with the highest precipitates (50F-50C and 50P-50C) at ambient conditions were subjected to 120 ºF and 2200 psi high temperature, high pressure, HPHT respectively. The result is presented in figure 3.18 as a comparison to ambient conditions. There is a slight decrease in Ph at HTHP, whiles turbidity drops. However, ζ-potential increase at reservoir conditions.

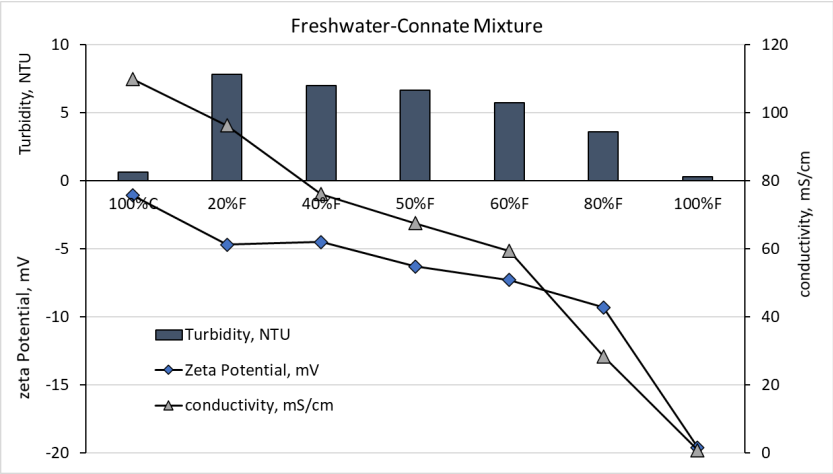

Figure 5(b): Turbidity, ζ-potential, and conductivity readings for LS (SIIW) and HS (SCW) mixtures

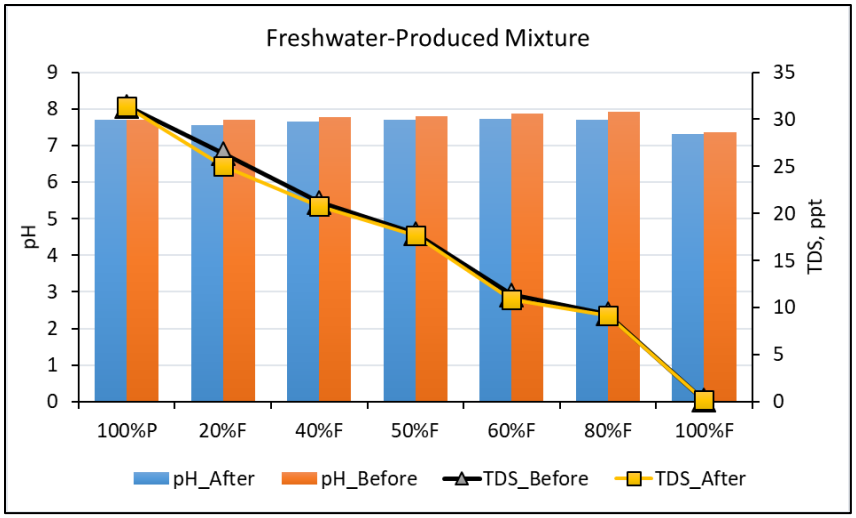

Figure 6(a): PH and TDS readings for LS (SIIW) and (SPW) mixtures

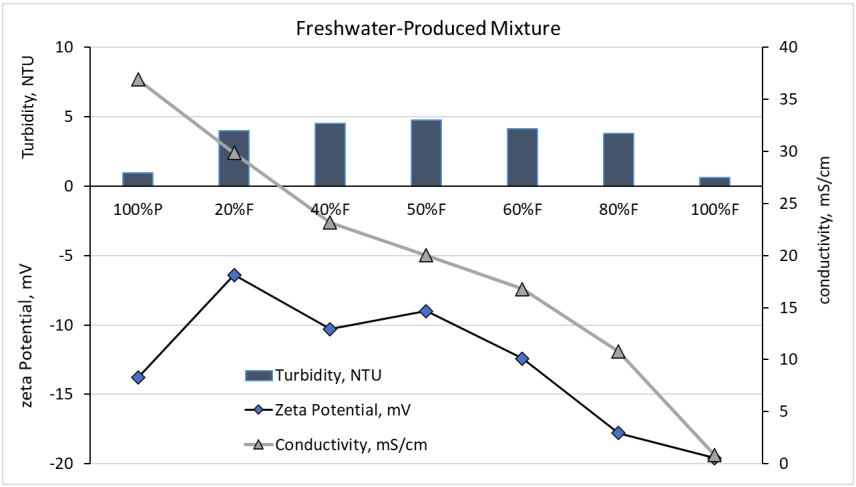

Figure 6(b): Turbidity, ζ-potential, and conductivity readings for LS (SIIW) and (SPW) mixtures

4.2 Rock – Fluid surface charge and electrical conductivity

Powdered samples from five core samples with different synthetic brines were mixed. Two samples were mixed with SPW, two with SIIW, and one with SCW. The pH values before and after mixing showed slight differences for all samples. The ζ-potential measurement showed a significant increase in all samples, except for the one mixed with SCW brine. The conductivity of all samples reduced as compared to the values of the original brine. Detailed results of rock-brine surface charge and electrical conductivity measurements are presented in Figure 19.

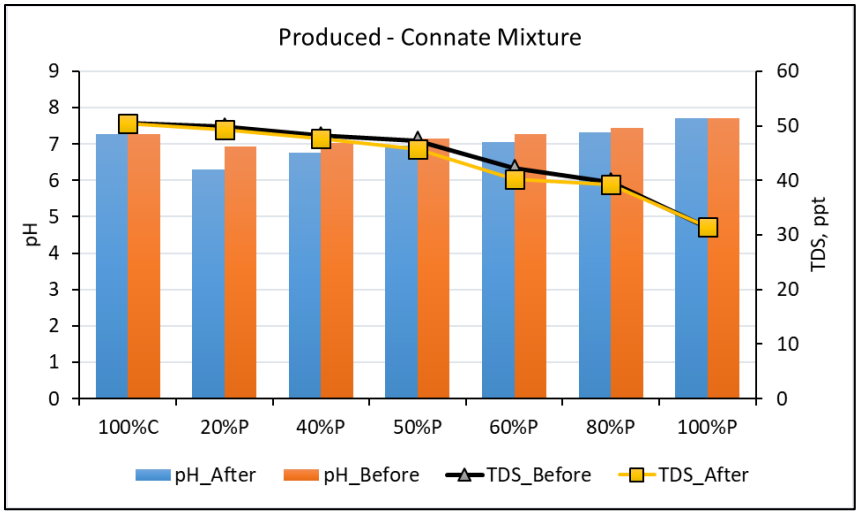

Figure 7(a): PH and TDS readings for SPW and SCW mixtures

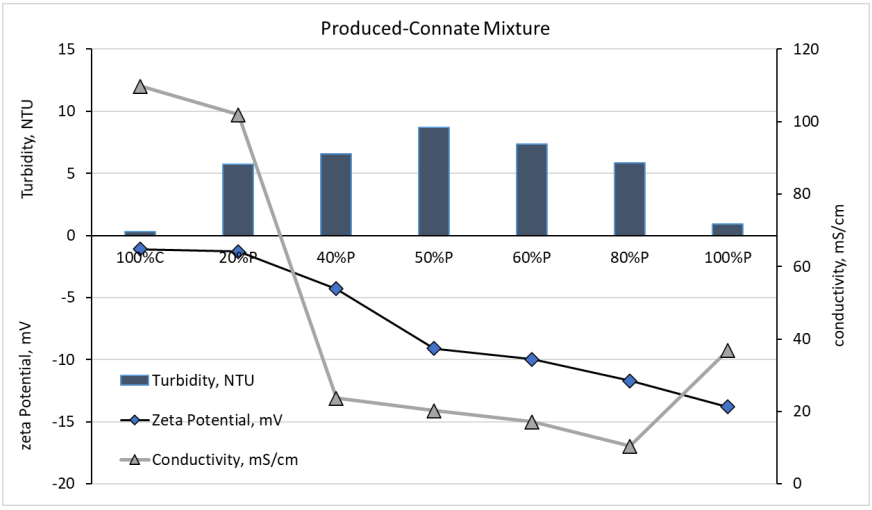

Figure 7(b): Turbidity, ζ-potential, and conductivity readings for SPW and SCW mixtures

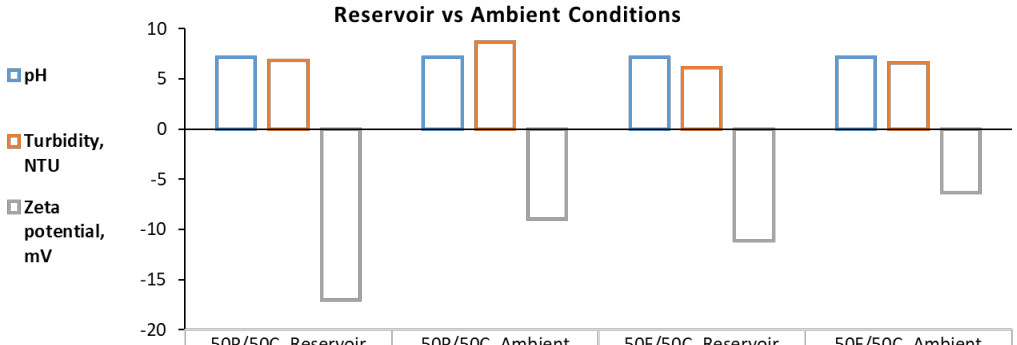

	50P/50C_Reservoir	50P/50C_Ambient	50F/50C_Reservoir	50F/50C_Ambient
pH	7.11	7.15	7.12	7.17
Turbidity, NTU	6.84	8.676	6.123	6.616
Zeta potential, mV	-17	-9	-11.13	-6.3

Figure 8: Comparative analysis of Turbidity, ζ-potential and Ph at ambient and reservoir conditions

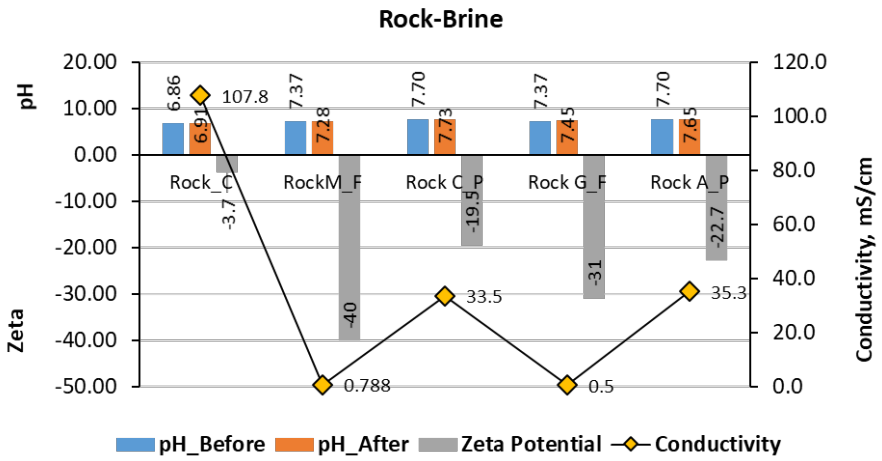

Figure 9: Rock-fluid surface chemistry and electrical conductivity

4.3 Brine geochemical Speciation reactions

Geochemical reactions of synthetic brine representing the FWU brine properties were further analyzed using PHREEQC. The workflow in Figure 2 was employed. Initial speciation of the 3 synthetic brines (SCW, SIIW, and SPW) were first modeled to confirm self-precipitation due to the non-zero turbidity measurements recorded for original brine. SIIW solution recorded saturation index (SI, Equation 1) of negative for all possible mineral formations based on its ionic composition at both ambient and reservoir conditions (Figure 10a). A negative SI indicates dissolution of all minerals and a positive indicate precipitation. The degree of dissolution or precipitation (undersaturation or over-saturation) however, depends on the magnitude of SI value and the conditions and factors favoring forward or backward reactions of the particular mineral based on the Le Chatelier's principle (concentration, temperature and pressure). As evident in turbidity measurement, SCW speciation analyzed showed some level of aragonite ($CaCO_3$), calcite ($CaCO_3$) and dolomite ($CaMg(CO_3)_2$ precipitates at both ambient and reservoir conditions (Figure 10b). SPW also recorded gibbsite ($Al(OH)_3$) and Alunite ($KAl_3(SO_4)_2(OH)_6$) precipitate together with mentioned minerals in SCW (Figure 10c).

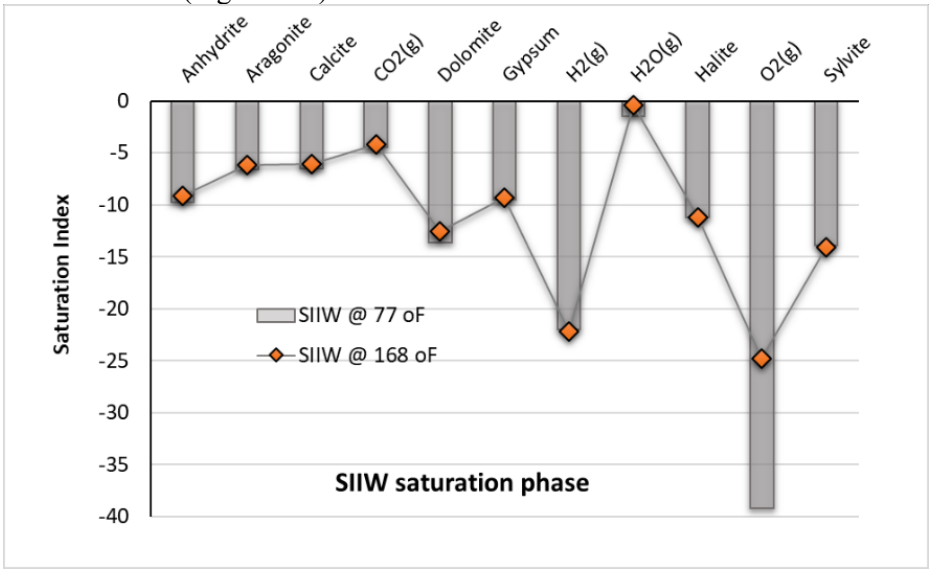

Figure 10(a): Chemical speciation of SIIW.

$$Saturation\ Index\ (SI) = log\left(\frac{IAP}{Ksp}\right) \qquad (1)$$

Where IAP is the ion activity product of dissolved species and Ksp is the solubility product constant of interested substances. A positive SI indicates concentration of a substance is greater than the solution's solubility hence the higher positive the SI the higher tendency of precipitation and vice versa for a negative SI, which represents solubility, where a very low negative means the solution has great capacity to dissolve substances. Geochemical model involved reactions between mixtures of the three brines at variable volume proportions at ambient and reservoir conditions. Three sets of principal mixtures were evaluated: SIIW – SCW, SIIW – SPW and SPW – SCW mixtures. Nine (9) mixtures were modeled for each of the sets varying at 10% by volume in each phase. Figures 11(a, b, c) present results and descriptions for each set.

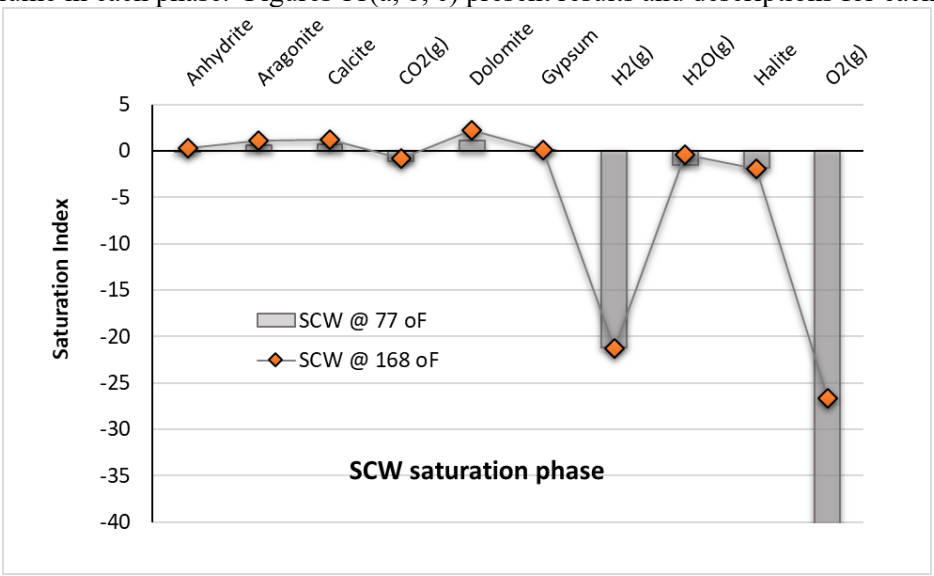

Figure 10(b): chemical speciation of SCW.

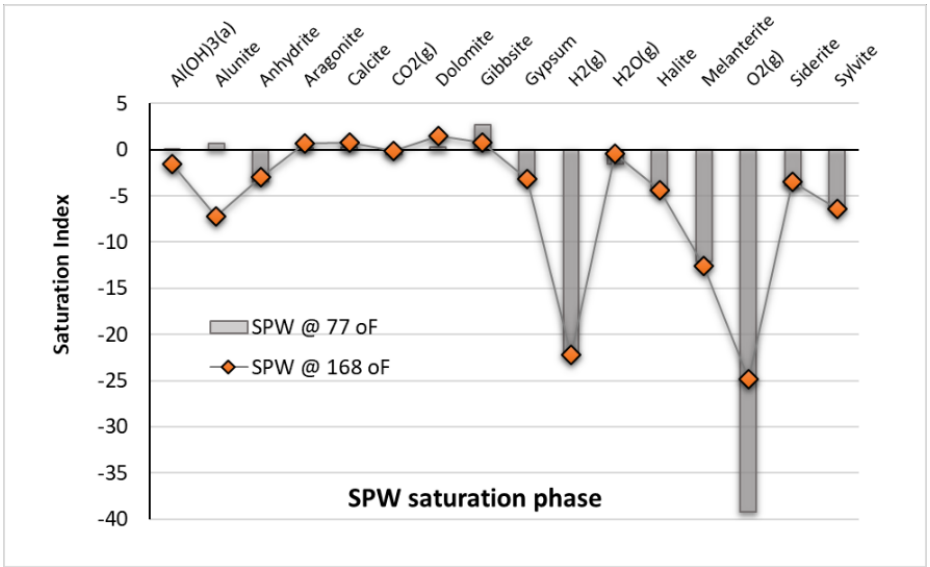

Figure 10c: Chemical speciation of SPW.

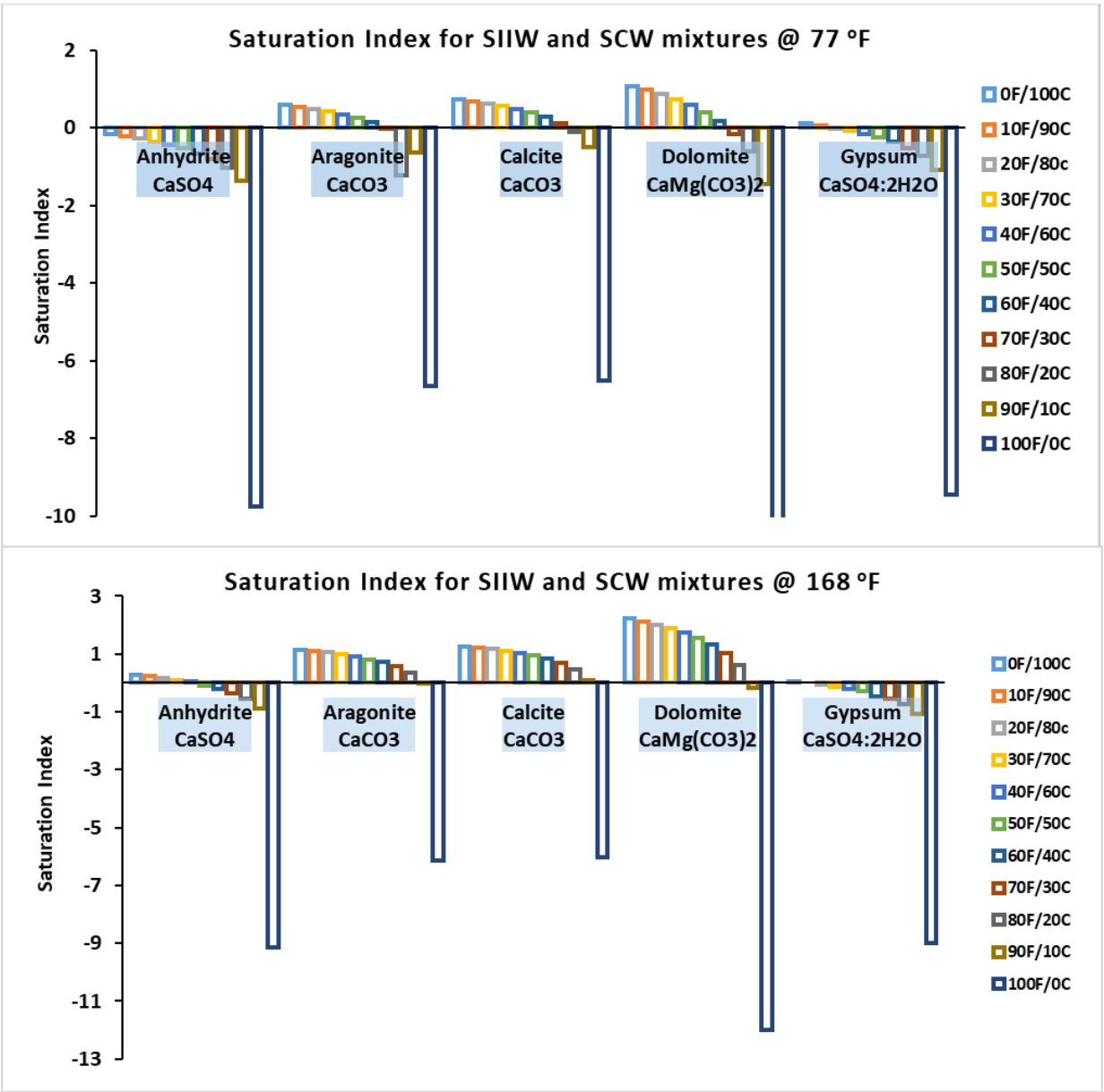

Figure 11 (a). geochemical reaction between SIIW and SCW. At ambient (77 ^{0}F) and reservoir, the major precipitates produced were carbonates. However, SI reduced as SIIW volume increased in all minerals until 70% SIIW (for 77 ^{o}F) and 90% SIIW for 168 ^{o}F, where all carbonates went into dissolution. SI for 168 Of were relatively higher. This indicates higher temperature and high concentrations of carbonate mineral ions favors their precipitation. At higher volumes of SCW (90%-50%) and higher temperature anhydrite recorded a positive SI.

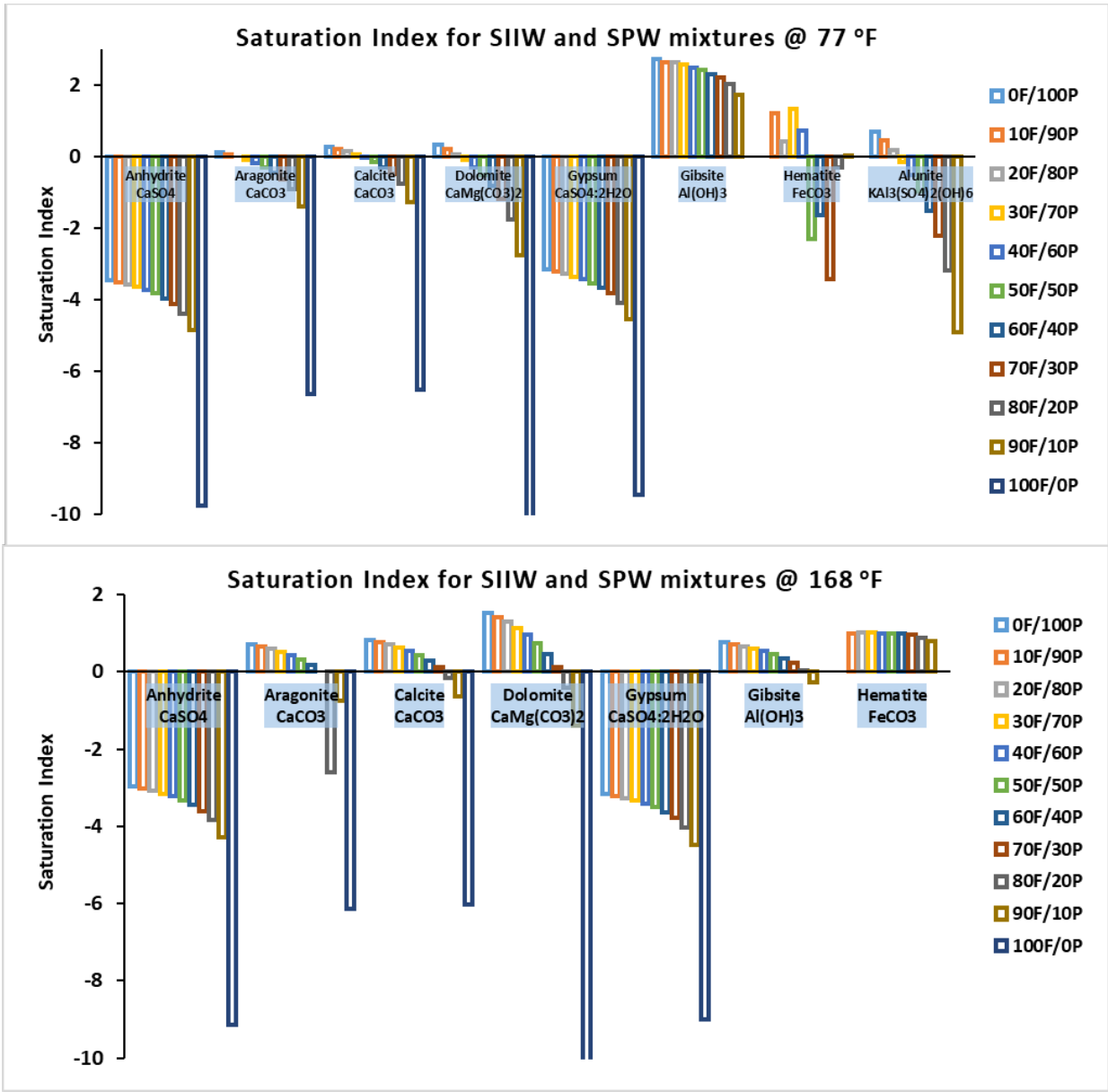

Figure 11(b). Brine geochemical reaction between SIIW and SPW at ambient and reservoir conditions. At ambient conditions (77 °F), all $CaSO_4$ mineral types are in dissolution. Carbonates as compared to SIIW and SCW have very low positive SI and reaction move to dissolution much faster (just about 30% volume of SIIW). However, the reaction favors gibbsite precipitation throughout the mixtures. Hematite and Alunite also precipitate until 40% of SIIW. Conversely, at reservoir conditions SI values for carbonates positively increases but reduces as volume of SIIW increase until at 70% when reaction shifts to dissolution. $CaSO_4$ and alunite remain in dissolution. Gibbsite reduces and dissolves at 90% SIIW and hematite precipitates at in all mixtures. This mixture is much more driven by temperature than concentration as seen in the results. Hence more precipitation is expected in the reservoir.

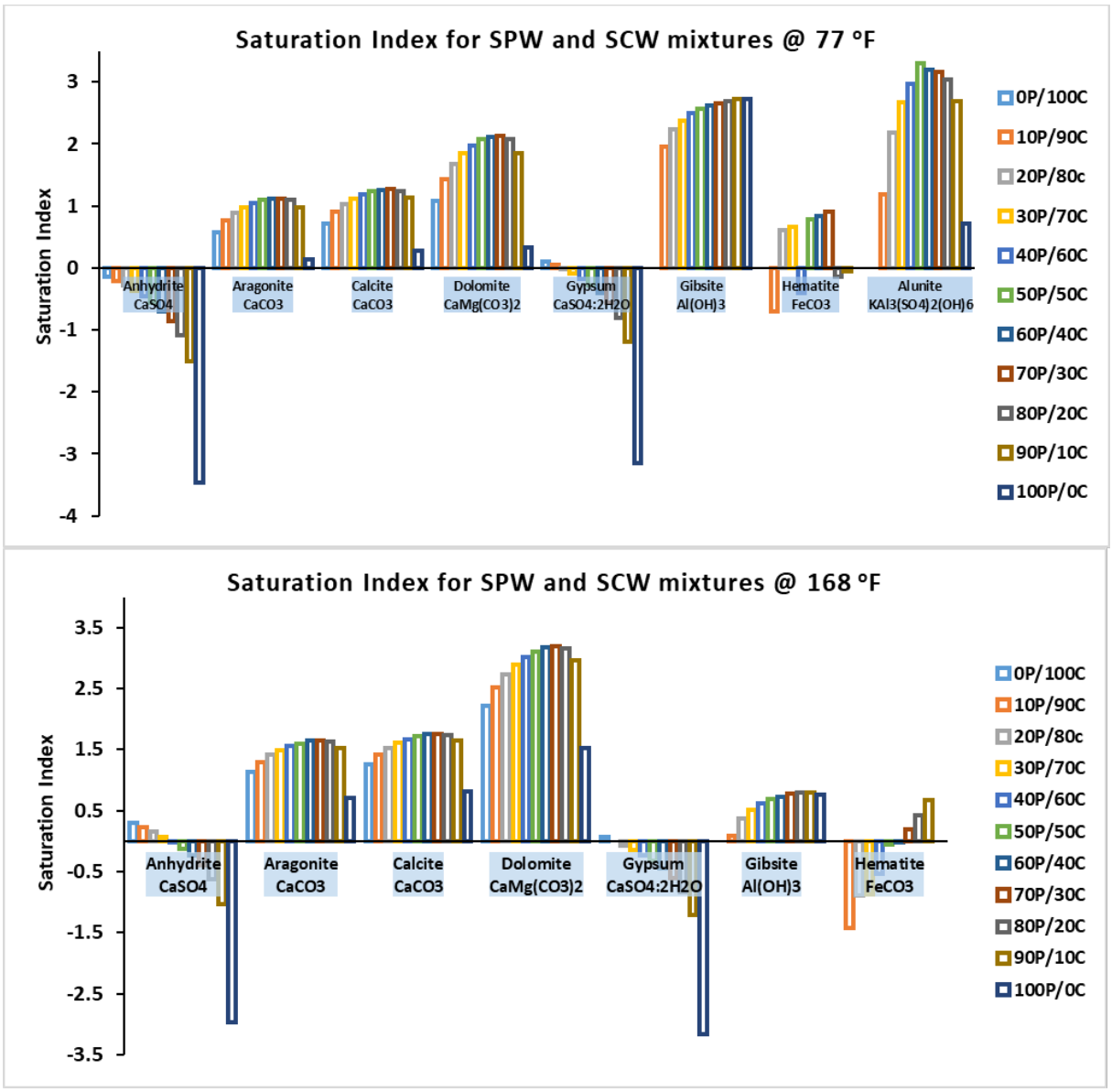

Figure 11(c). Brine geochemical reaction between SPW and SCW. SCW is highly concentrated with cations (Na, Mg and Ca) and SCW is relatively concentrated with more different cations (Na, Mg, Ca, Al, K, and Fe). From the results at both ambient and reservoir conditions ionic concentrations play a key condition for the precipitation of carbonates. However, temperature also had a significant role by increasing the SI of carbonates at reservoir conditions as seen in other mixtures described above. The influence of temperature also caused the dissolution of alunite completely at reservoir conditions. Gypsum and it related minerals are almost always in dissolution. This can be due to the low concentration of SO_4 ions in all brine compositions.

5.0 Discussions

Development of a successful improved recovery technique after a reservoir is flooded with water (secondary recovery) will largely depend on the outcome of waterflood implementation. It is imperative that the mechanisms responsible for inefficiency or failure of waterflood be investigated. Through experimental approach, the cause of inefficiency on FWU-east is assessed. This chapter provides detailed

analysis of results from the test outcomes from the experiments conducted and how they explain the mechanisms responsible for the poor outcome of waterflood.

5.1 Injectant and connate water salinities and surface charge implications during waterflood at FWU-East

The potential impact of injection water on reservoir fluids and rock, which includes adverse reactions or precipitation can cause detrimental issues in the reservoir with associated production issues and challenges. Previous sections have addressed rock-fluid interaction and implications on reservoir quality. This section discusses results of fluid-fluid interaction and compatibility assessment. Both physical (mixing fluids and observing for phase separation, turbidity or precipitates) and chemical (pH, electrical conductivity, TDS and ζ-potential) compatibility tests were conducted. Geochemistry speciation and reaction simulation with PHREEQC was further conducted to confirm results of laboratory tests. Formation of precipitates or scale formation may occur when the amount of certain minerals in solution exceed solubility limit, mixing of solutions with incompatible ionic constituents and changes in pressure and temperature conditions.

5.2 Compatibility and surface charge of brine at ambient conditions

Three brine solutions, including SCW, SPW and SIIW, were considered for compatibility testing. Turbidity measurements of all mixtures indicated low levels of precipitation as all values for all mixtures were below 10 NTU at ambient condition (Figures 5b, 6b & 7b). The highest recorded value was 8.7 NTU for a mixture of 50% SPW and 50% SCW. After 7 days, precipitation, pH, TDS and conductivity reduction was recorded for all mixtures (Figures 5a, 6a & 7a). This supports that precipitation occurred. Precipitation will lead to the increase in H+ ions and reduction in cations (Ca2+, Mg2+) concentrations as these minerals are formed. As H+ ions increase with a reduction in principal cations in solution, pH declines, TDS reduces with a corresponding decrease in electrical conductivity, which is based on the ionic concentration of the mixtures.

Turbidity reduces as percentage of SIIW (LS) volume increases for SIIW and SCW mixtures (Figure 5b). This occurs with a corresponding increase in negative surface charge (ζ potential) (Figures 5b). The (ζ potential) of 100% SCW is -1.1 Mv and 100% SIIW-LS is -19 Mv. This means that SIIW has stronger electrostatic forces (stable solution) keeping brine particles from aggregating, whereas SCW has a weak electrostatic force and an unstable solution. Thus, in mixing these two solutions, where SIIW has HCO^{3-} as the highest ionic composition, the likelihood of precipitation reactions with SCW (high salinity with highest cationic concentration) occurs, and as the volume of SIIW mixture increases, SCW reduces, diminishing the number of cations in solution. Hence, a decrease in precipitation and a gradual increase in negative surface charge (ζ potential) of the resulting solution as observed in the geochemical reaction analysis in Figure 11a. This leads to reduction in cations and carbonate ions with an increase H+ ions leading to pH, TDS and conductivity reduction. In this case, interaction between LS-SIIW and SCW ions alters the electrostatic properties and stability of suspended particles in the final mixture. This disrupts the equilibrium and repulsive forces between particles which enhances aggregation or flocculation.

Mixing SIIW and SPW relatively recorded lower turbidity as compared to SIIW and SCW mixtures. This can be attributed to the more stable electrostatic forces (ζ potential = -13 Mv) of SPW brine than those of SCW (-1.1 Mv). Also from geochemical analysis, there was less carbonate formation, which went into dissolution at 50% SIIW and beyond (Figure 11b). In the case of this mixture, as volume percent of LS increases the turbidity increases with a decrease in ζ-potential; but as volume of LS exceeds 50%, the turbidity reduces with an increase in negative ζ-potential (Figure 6b). Low concentration of LS ion creates instability in the electrostatic force of the mixture leading to a low ζ-potential resulting in the formation of larger aggregates, hence an increase in turbidity. However, LS alters the chemical composition of the mixture as it reaches a certain optimal concentration threshold (above 50%). This leads to the surface complexes and precipitation reaction causing the formation of much larger rapidly settling particles with

different surface properties and surface charges causing an increase in ζ-potential. Electrostatic force by virtue of increase in ζ-potential is also increased and hence particle repulsion creating a reduction in turbidity. Complex precipitation reactions and changes to the properties of particles are a result of excess in LS volume. However, geochemical analysis shows a drop in all carbonate precipitations at about 50% of SIIW, an indication of reduced carbonate forming ions hence less turbidity and high stability (ζ-potential).

The highest turbidity measurements were recorded in the SPW and SCW mixtures (figure 7b), apparently because of the relatively higher ionic concentrations in both solutions, which favored precipitation as shown in geochemical reaction (Figure 11c). Turbidity however followed the same trend as described in SIIW and SPW mixtures. ζ-potential increased as percentage volume of SPW increased. This is due to the fact that SPW relatively had a higher ionic concentration to undergo surface complexes and precipitation reaction causing the formation of much larger rapidly settling particles with different surface properties and surface charges causing an increase in ζ-potential. Geochemical reactions highlights drop in SI values as volume of SPW increases beyond 50% except gibbsite. Presented in Figures 12(a, b & c) are the summarized geochemical signatures of mixtures considered.

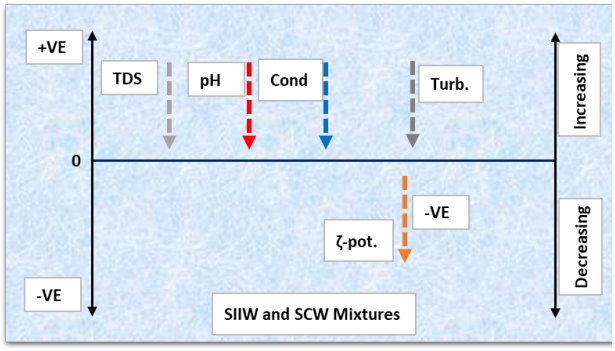

Figure 12(a): SIIW and SCW

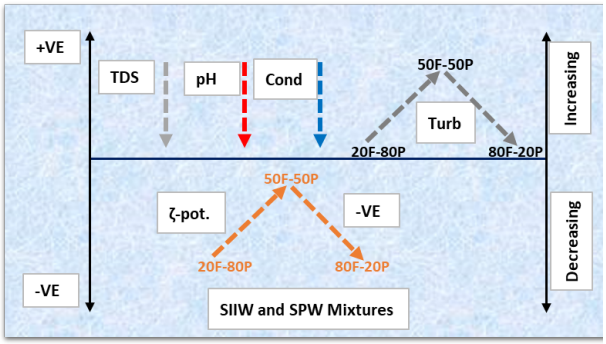

Figure 12(b): SIIW and SPW

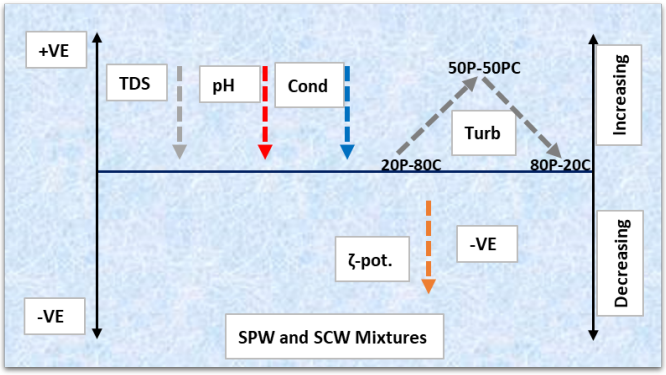

Figure 12(c): SPW and SCW

Figures 12(a) & 12(b) are Geochemical reaction signature of mixtures with increasing proportion of SIIW and Figure 12(c) is with respect to increasing SPW

5.3 Compatibility and surface charge tests at HTHP conditions

Two mixtures comprising 50% SIIW/50% SCW and 50% SPW/50% SCW were subjected to HTHP (120 ^{o}F and 2200 psi) to assess the effect of HTHP on compatibility since these conditions favor calcite, dolomite and gypsum precipitation. Note that siderite forms at lower temperatures. As observed at ambient conditions, pH reduction was also observed (Figure 12). Turbidity recorded for 50% SPW/50% SCW mixture at reservoir reduced (about 21% reduction) with a corresponding increase in ζ-potential. At HTHP, certain precipitates were not favored. Rather, the reaction equilibrium favored dissolutions of these ions

leading to a relatively stronger repulsive electrostatic force. The mixture involving 50% SIIW/50% SCW also recorded a slight 7.5% decrease in turbidity with an increase in ζ-potential. Geochemical analysis shows an increased precipitation for carbonates, as HTHP conditions favors precipitation (Figures 11a-11c @ 168 ^{o}F). Conversely, gibbsite saw a great reduction in SI values. Generally, there was a reduction as volume of lowest ionic concentrated brine increased.

One key observation is that, the precipitation reaction (based on turbidity measurement) is dictated by the original ζ-potential or surface charge magnitude of the original solutions forming the mixtures and greatly by the ionic strength or proportion (volume) of each solution forming the mixture. Fluid incompatibility based on turbidity and SI values as well as ζ-potential are relatively low for synthetic FWU-east connate brine, produced brine and initial injection water (fresh water from Ogallala River). The severity as observed occurs when the volume of the least concentrated brine is low, which means precipitation occurs in the early start of injection but as injection volume increases precipitation reduces. However, the early adverse effect can lead to formation damage causing injectivity and flow issues.

5.4 Rock-brine surface chemistry: Insight from surface charge and electrical conductivity tests

As described in Figure 9, five rock samples were used to conduct surface chemistry interaction test with synthetic brine. Changes in pH measurement indicates surface reactions between the rock and brine. SCW sample (RockC) with -3.7 Mv is the ζ-potential least change from the original value of -1.1 Mv. This was expected as an indication of low surface reactivity since it represents the connate water saturation at initial reservoir phase. Produced water (SCW) also had an increase in ζ-potential (RockC_P and RockA_P) which shows some level of geochemical surface reaction, however low salinity water (SIIW) mixed with samples RockM_F and RockG_F recorded the highest ζ-potential. This is an indication of high surface activity between low salinity and rock minerals especially clay minerals. Table 3, summarizes various inferences that can be gathered from the results.

Table 3: Rock-brine surface chemistry and inferences gathered.

Activity	Inference
Ion Exchange and Surface Chemistry	Increase or decrease in ζ-potential indicates changes in concentration of adsorbed ions or surface charge behavior due to interaction with SIIW. Ionic exchange and surface reaction which lead to release of more ions into the solution charged the electrostatic forces hence the increase in ζ-potential.
Dispersion or Aggregation	Higher electrostatic forces as a result of ionic exchange between rock and SIIW brine indicates high repulsion between particles. This means clay particle is more dispersed and less tendency for aggregation or settling hence highly mobile. This mobility in a very low permeable reservoir as FWU-east leads to pore plugging.
Reduced Scaling Tendency	Stronger electrostatic forces lead to high repulsion tendencies. This implies that particles have reduced susceptibility for mineral deposition and scaling potential preventing precipitation.
Wettability Alteration	Surface charge properties of rocks due to ionic exchange with low salinity can be changed. This affects wettability of the rock surface. Low salinity through ionic exchanges and dissolution leads to a higher ζ-potential which is linked to a shift in wettability to more water wet. This is one of the major mechanisms reported in the recovery of oil by low salinity flooding. This leads to the release of rock minerals, clays especially which may lead to reservoir impairment for low permeable reservoirs.
Enhanced Fluid and mineral Flow	When ζ-potential increases, it can lead to better fluid and mineral flow. This is because higher values of ζ-potential mean more electrostatic repulsion between particles, making it easier for them to flow through the rock. It appears that a low salinity brine may have changed the surface properties of the rock, resulting in

	improved flow characteristics. However, if a reservoir has many micro pores or low permeability, there is a risk of particles building up and blocking the flow in the long term.

6.0 Conclusions

This study aimed to investigate the primary factors contributing to the inefficiency of waterflooding in the FWU-east and to provide insights to the development of further improved recovery technique (specifically CO_2-WAG EOR). To achieve this objective, a series of experiments were conducted encompassing core-flood experiments involving the injection of single-phase brine. Furthermore, tests were carried out to evaluate fluid-fluid surface charge, compatibility, and the surface chemistry analysis of rock-fluid interactions. Various parameters were measured and analyzed, including pH, TDS, electrical conductivity, surface charge, electrostatic stability (ζ-potential), turbidity, differential pressure, flow and storage capacities.

The study highlights that the east section of the field has notably lower permeability than the west section. Preliminary analysis also detects the presence of authigenic clays in FWU[22]. Geochemical analysis indicates both fluid-fluid and rock-fluid reactivity (incompatibility) between the formation and the injected water. This reactivity has the potential to induce pore plugging, resulting in a reduction of flow capacity. Given the very low permeability on the east side, there is a higher susceptibility to formation impairment and inefficient flooding compared to the west. The study presents various geochemical signatures, providing valuable insights. This understanding can significantly enhance the engineering of the appropriate brine composition for CO2-WAG operations in subsequent studies.

Acknowledgement: Funding for this project is provided by the U.S. Department of Energy's (DOE) National Energy Technology Laboratory (NETL) through the Southwest Regional Partnership on Carbon Sequestration (SWP) under Award No. DE-FC26-05NT42591.

References

[1] V. K. Kudapa and K. A. Suriya Krishna, "Heavy oil recovery using gas injection methods and its challenges and opportunities," *Mater. Today Proc.*, 2023, doi: https://doi.org/10.1016/j.matpr.2023.05.091.

[2] S. Chen, H. Li, D. Yang, and P. Tontiwachwuthikul, "Optimal Parametric Design for Water-Alternating-Gas (WAG) Process in a CO2-Miscible Flooding Reservoir," *J. Can. Pet. Technol.*, vol. 49, no. 10, pp. 75–82, Oct. 2010, doi: 10.2118/141650-PA.

[3] M. M. Kulkarni and D. N. Rao, "Experimental investigation of miscible and immiscible Water-Alternating-Gas (WAG) process performance," *J. Pet. Sci. Eng.*, vol. 48, no. 1, pp. 1–20, 2005, doi: https://doi.org/10.1016/j.petrol.2005.05.001.

[4] C. Anthony, Morgan; William, Ampomah; Reid , Grigg; Sai, Wang; Robert, "Experimental Investigation Of Waterflood Performance Challenges In A Low-Permeability Morrowan Sandstone Reservoir: Implications For Mechanistic Modeling And Enhanced Oil Recovery Optimization," 2024, doi: SPE-218876-MS.

[5] C. Anthony, Morgan; William, Ampomah; Reid , Grigg; Sai, Wang; Robert, "Unveiling The Enigma Of Waterflood Inefficiency: A Multifaceted Analysis Of Geological, Petrophysical, And Reservoir Dynamics - A Case Study In A Morrowan Clastic Reservoir," 2024, doi: SPE-218943-MS.

[6] J. You *et al.*, "Machine learning based co-optimization of carbon dioxide sequestration and oil

recovery in CO2-EOR project," *J. Clean. Prod.*, vol. 260, p. 120866, Mar. 2020, doi: 10.1016/j.jclepro.2020.120866.

[7] W. Ampomah, R. S. Balch, R. B. Grigg, R. Will, Z. Dai, and M. D. White, "Farnsworth Field CO2-EOR Project: Performance Case History," *SPE Improved Oil Recovery Conference*. Society of Petroleum Engineers, Tulsa, Oklahoma, USA, p. 18, 2016, doi: 10.2118/179528-MS.

[8] A. Morgan, R. Grigg, and W. Ampomah, "A Gate-to-Gate Life Cycle Assessment for the CO2-EOR Operations at Farnsworth Unit (FWU)," *Energies* , vol. 14, no. 9. 2021, doi: 10.3390/en14092499.

[9] W. Ampomah, R. S. Balch, R. B. Grigg, Z. Dai, and F. Pan, "Compositional Simulation of CO2 Storage Capacity in Depleted Oil Reservoirs," *Carbon Management Technology Conference*. Nov. 17, 2015, doi: 10.7122/439476-MS.

[10] J. You, W. Ampomah, A. Morgan, Q. Sun, and X. Huang, "A comprehensive techno-eco-assessment of CO2 enhanced oil recovery projects using a machine-learning assisted workflow," *Int. J. Greenh. Gas Control*, vol. 111, p. 103480, 2021, doi: https://doi.org/10.1016/j.ijggc.2021.103480.

[11] M. Cather *et al.*, "Deposition, Diagenesis, and Sequence Stratigraphy of the Pennsylvanian Morrowan and Atokan Intervals at Farnsworth Unit," *Energies* , vol. 14, no. 4. 2021, doi: 10.3390/en14041057.

[12] A. Morgan, W. Ampomah, R. Grigg, Z. Dai, J. You, and S. Wang, "Techno-economic life cycle assessment of CO2-EOR operations towards net negative emissions at farnsworth field unit," *Fuel*, vol. 342, p. 127897, 2023, doi: https://doi.org/10.1016/j.fuel.2023.127897.

[13] W. Ampomah, R. S. Balch, R. B. Grigg, Z. Dai, and F. Pan, "Compositional Simulation of CO2 Storage Capacity in Depleted Oil Reservoirs," *Carbon Management Technology Conference*. Nov. 2015, doi: 10.7122/439476-MS.

[14] T. W. Munson, "Depositional, diagenetic, and production history of the Upper Morrowan Buckhaults Sandstone, Farnsworth Field, Ochiltree County Texas," *Shale Shak.*, pp. 1–19, 1989.

[15] Swanson, D., "Deltaic Deposits in the Pennsylvanian upper Morrow Formation in the Anadarko Basin, in Pennsylvanian sandstones of the mid-continent," *Tulsa Geol. Soc. Spec. Publ.*, vol. 1, pp. 115–168, 1979.

[16] J. Puckette, Z. Al-Shaieb, E. Van Evera, and R. D. Andrews, "Sequence stratigraphy, lithofacies, and reservoir quality, upper Morrow sandstones, northwestern shelf, Anadarko Basin," in *Morrow and Springer in the southern midcontinent, 2005 symposium: Oklahoma Geological Survey Circular*, 2008, no. 111, pp. 81–97.

[17] P. Bowen, D. W., & Weimer, "Reservoir geology of Nicholas and Liverpool cemetery fields (lower Pennsylvanian), Stanton county, Kansas, and their significance to the regional interpretation of the Morrow Formation incised-valley- fill systems in eastern Colorado and western Kansas," *Am. Assoc. Pet. Geol. Bull.*, vol. 88, no. 1, pp. 47–70, 2004, doi: http://doi.org/10.1306/09100301132.

[18] A. A. DeVries, *Sequence stratigraphy and micro-image analysis of the upper Morrow sandstone in the Mustang East field, Morton County, Kansas*. Oklahoma State University, 2005.

[19] S. R. Gallagher, "Depositional and diagenetic controls on reservoir heterogeneity: upper morrow sandstone, Farnsworth unit, Ochiltree county, Texas." Citeseer, 2014.

[20] P. A. Dickey and C. Soto, "Chemical composition of deep subsurface waters of the western anadarko basin," *Soc. Pet. Eng. - SPE Deep Drill. Prod. Symp. DDPS 1974*, pp. 111–127, 1974,

doi: 10.2118/5178-ms.

[21] E. J. Kutsienyo, “Three Phase Compositional Reservoir Simulation Model Coupled with Reactive Transport for CO2 Storage in the Farnsworth Unit, Ochiltree County, Texas,” New Mexico Institute of Mining and Technology PP - United States -- New Mexico, United States -- New Mexico, 2019.

[22] R. C. A. Morgan, W. Ampomah, R. Grigg, S. Wang, “Unveiling the Enigma of Waterflood Inefficiency: A Multifaceted Analysis of Geological, Petrophysical, and Reservoir Dynamics - A Case Study in a Morrowan Clastic Reservoir,” 2024, [Online]. Available: SPE-218229-MS.